Glutathione disulfide induces neural cell death via a 12-lipoxygenase pathway

Han-A Park, **Savita Khanna**, **Cameron Rink**, **Surya Gnyawali**, **Sashwati Roy**, and **Chandan K. Sen**

Departments of Surgery, Davis Heart and Lung Research Institute, The Ohio State University Medical Center, Columbus, Ohio 43210

Abstract

Oxidized glutathione (GSSG) is commonly viewed as a byproduct of GSH metabolism. The pathophysiological significance of GSSG *per se* remains poorly understood. Adopting a microinjection approach to isolate GSSG elevation within the cell, this work identifies that GSSG can trigger neural HT4 cell death *via* a 12-lipoxygenase (12-Lox) dependent mechanism. *In vivo*, stereotaxic injection of GSSG into the brain caused lesion in wild-type but less so in 12-Lox knockout mice. Microinjection of graded amounts identified 0.5mM as the lethal [GSSG]i in resting cells. Interestingly, this threshold was shifted to the left by 20-fold (0.025 mM) in GSH-deficient cells. This is important because tissue GSH lowering is commonly noted in the context of several diseases as well as in aging. Inhibition of GSSG reductase by BCNU is known to result in GSSG accumulation and caused cell death in a 12-Lox sensitive manner. GSSG S-glutathionylated purified 12-Lox as well as in a model of glutamate-induced HT4 cell death *in vitro* where V5-tagged 12-Lox was expressed in cells. Countering glutamate-induced 12-Lox S-glutathionylation by glutaredoxin-1 overexpression protected against cell death. Strategies directed at improving or arresting cellular GSSG clearance may be effective in minimizing oxidative stress related tissue injury or potentiating the killing of tumor cells, respectively.

Introduction

Free glutathione, a tripeptide with the sequence γ-Glu-Cys-Gly, exists either in a reduced form with a free thiol group (GSH) or in an oxidized form with a disulfide between two identical molecules (GSSG). GSH is a ubiquitous low molecular weight intracellular thiol present in all aerobic cells in millimolar concentrations. The sulfhydryl (-SH) group supports the reducing properties of GSH by way of a thiol-exchange system (-SH to -S-S-), making GSH one of the most abundant and powerful intracellular antioxidants. Besides scavenging free radicals and reactive oxygen species, GSH detoxifies tissues by conjugating with various electrophiles including xenobiotics. In addition, GSH serves as a major reservoir of cysteine for cellular protein synthesis.

Address correspondence to: Prof. Chandan K Sen 512 Davis Heart & Lung Research Institute 473 West 12th Avenue The Ohio State University Medical Center Columbus, Ohio 43210 Tel. 614 247 7658, Fax 614 247 7818.

Under basal conditions, GSSG represents 1% of the total GSH in the cell (1). Under conditions of oxidant insult, GSH is rapidly oxidized to GSSG. Thus, an elevated GSSG/GSH ratio is often used as a marker for oxidative stress (2). Cellular GSSG may be recycled to GSH in the presence of reductases such as NADPH-dependent GSSG reductase. Excessive GSSG, as generated during sudden oxidant insult, is pumped out of the cell by a ATP-dependent process underscoring the urgent need of the cell to protect itself from a GSSG surge (3, 4). In most studies, GSSG is dealt with as a byproduct of GSH metabolism. Because cellular GSH concentration is expected to be in the range of 1–5 mM, millimolar concentrations of GSSG are expected in cells under conditions of oxidant insult. However, knowledge about the potential biological significance of GSSG *per se* is limited. While excessive oxidant insult causes necrotic cell death, a more moderate challenge triggers secondary responses in the cell that culminate in cell death. Elevation in cellular GSSG levels represents one such rapid cellular response to moderate oxidant insult. In this study, we sought to examine whether elevated cellular GSSG levels may directly influence cell death. Addressing this question would require that cellular GSSG elevation be isolated from all other biological causative factors. Thus, we adopted the microinjection approach (5) to raise cellular GSSG or GSH as control to investigate the significance of GSSG on cell death. To test the significance of our findings *in vitro*, GSSG was stereotaxically injected to the brain *in vivo* and MRI was performed to quantify tissue lesion.

Results

Increased extracellular glutamate depletes intracellular GSH (5, 6). To test the significance of this loss of cellular GSH during glutamate-induced loss of HT4 cell viability, GSH was replenished in glutamate-treated cells by microinjection. Previously we have reported that 4h of glutamate treatment markedly depletes the cellular GSH pool (6, 7). Thus, 4h glutamate treatment was performed in these experiments. After 4h of treatment, glutamate was withdrawn and cell were microinjected with GSH. Because the antioxidant properties of GSH were being tested, GSSG was selected as control. GSH microinjection did not significantly rescue cells from glutamate-induced death. This observation was consistent with our previous indirect observation that glutathione depletion is not critically important in causing cell death because we were previously able to afford complete protection by the α-tocotrienol form of natural vitamin E under conditions where glutamate-induced glutathione loss remained unaffected (6). Of striking interest, however, was the observation that the control cells microinjected with GSSG were all lost to death. GSSG microinjection proved to be potently cytotoxic (Fig. 1). This serendipitous observation led us to examine the threshold of intracellular GSSG concentration ([GSSG]i) that triggers cell death of HT4 neural cells. Based on atomic force microscopy measurements, we determined that the mean HT4 cell volume is in the order of 1 pl (not shown). Microinjection of graded amounts of GSSG was performed to identify the threshold concentration of GSSG that trigger cell death. It was noted that injection of 500 attomoles of GSSG which is equivalent to 0.5 mM of [GSSG]i was the threshold at which GSSG caused death of HT4 cell under standard culture conditions (Fig. 2A). Under conditions of glutamate challenge or other insult leading to cell death, cellular GSH levels are known to sharply fall (6). Therefore, we chose to lower GSH levels in cells by arresting GSH synthesis using BSO. BSO sharply increased GSSG

levels (Fig. 2C) and depleted cellular GSH pool by 80% (Fig. 2D) similar to the magnitude noted during glutamate challenge (6). Under such GSH-depleted conditions, HT4 cells were noted to become more sensitive to GSSG-induced cell death. In such GSH-deficient cells, the threshold for GSSG-induced lethality was lowered by twenty-fold such that microinjection of 25 attomoles (corresponding to 0.025 mM) of GSSG caused cytotoxicity (Fig. 2B–D). These observations underscore the heightened significance of GSSG as an inducer of cell death under conditions of GSH depletion.

Characterization of GSSG-induced death of HT4 neural cells was started by testing the involvement of mitochondrial dysfunction as is commonly associated with cell death. Cytosolic injection of GSSG was observed to selectively compromise mitochondrial membrane potential while not affecting plasma membrane potential (Fig. 3). Previously, we had reported that GSH-depletion in glutamate-challenged HT4 neural cells leads to the activation of 12-lipoxygenase which is central in executing glutamate-induced neural cell death. Inhibitors of 12-lipoxygenase, including BL-15 and α-tocotrienol, prevent glutamate-induced HT4 cell death (5, 6). We therefore sought to examine whether GSSG-induced death of HT4 neural cells is mediated by 12-lipoxygenae. Both inhibitors of 12-lipoxygenase, BL-15 as well as α-tocotrienol, significantly protected against GSSG-induced loss of cell viability suggesting the involvement of 12-lipoxygenase in this death pathway (Fig. 4). Next, we utilized the advantages of the microinjection approach to test the significance of 12-lipoxygenase and its substrate arachidonic acid in the death of GSH-deficient HT4 cells. While depletion of cellular GSH reserves by arresting GSH synthesis using BSO does not cause cell death, such GSH-deficient cells are known to be highly sensitive to extracellular arachidonic acid treatment (5). Consistently, in this study we observed that microinjection of small amounts of free arachidonic acid to GSH-deficient HT4 cells caused cell death (Fig. 5). Both BL-15 as well as α-tocotrienol protected against such death suggesting the involvement of 12-lipoxygenase in intracellular free arachidonic acid induced cell death. Supporting this conclusion is our observation that direct administration of active 12-lipoxygenase into GSH-deficient cells causes cell death in a BL-15 and α-tocotrienol sensitive manner (Fig. 5). Next, we sought to test whether endogenous GSSG may kill cells by a 12-lipoxygenase dependent mechanism. BCNU, a well-characterized GSSG reductase inhibitor, was chosen as a pharmacological tool to increase cellular GSSG:GSH ratio (8, 9). Indeed, BCNU-induced elevation of cellular GSSG caused cell death. BCNU-induced cell death was significantly lowered by BL-15 as well as α-tocotrienol suggesting the involvement of 12-lipoxygenase (Fig. 6A–F). Inhibition of GSSG efflux by MK-571, an inhibitor for multidrug resistance protein-1 (MRP1)(10, 11), significantly increased loss of HT4 viability (Fig. 6G).

Consistent observations indicating that GSSG may induce cell death by a 12-lipoxygenase dependent mechanism led us to investigate the relationship between GSSG and 12-lipoxygenase. Using a standard assay to measure 12-lipoxygenase activity it was noted that the presence of GSSG in the reaction mixture significantly increases the catalytic function of 12-lipoxygenase (Fig. 7A). GSSG was noted to cause marked S-glutathionylation of proteins in HT4 cells (Fig. 7B). Control cells did show baseline glutathionylation levels (Fig. S1) but they are not noticed in Fig. 7B because film exposure time was minimized to obtain a good resolution blot of the GSSG treated cells. Signal detected as protein glutathionylation by

immunoblots was reversed under reducing conditions demonstrating specificity of the antibody used (Fig. S1). To determine whether 12-lipoxygenase is subject to GSSG-induced S-glutathionylation HT4 cells were transfected with vectors expressing V5-tagged 12-lipoxygenase. Cell lysates from such cells, containing V5-tagged 12-lipoxygenase, were incubated with GSSG. Interestingly, the formation of GSS-12-lipoxygenase was noted (Fig. 7C). Thus, G S S G is capable of S-glutathionylating 12-lipoxygenase. These findings were consistent with our observation that GSSG is able to S-glutathionylate pure 12-lipoxygenase obtained commercially (Fig. 7D).

Glutaredoxin 1(GRx1) is the most specific and efficient deglutathionylating enzyme in the cytoplasm of mammalian cells (12). To test the overall significance of S-glutathionylation on glutamate-induced cell death, HT4 cells were infected with an adenoviral vector expressing GRx1. The gene delivery process was successful in markedly increasing cellular GRx1 expression (Fig. 8A–C). Globally, GRx1 overexpression lowered the empirical abundance of S-glutathionylated proteins in the cell indicating elevated catalytic function of GRx1 in the cells (Fig. 8D). Overexpression of GRx1 significantly protected HT4 neural cells against glutamate challenge. These findings suggest the involvement of S-glutathionylation reactions in glutamate-induced cell death (Fig. 8E). To expand on the mechanism by which GRx1 may have protected the cells against glutamate-insult, S-glutathionylation of V5-tagged 12-lipoxygenase was examined in HT4 cells. Glutamate increased 12-lipoxygenase glutanthionylation which was prevented in GRx1 over-expressing cells (Fig. 8F). These findings were consistent with results from studies employing the microinjection approach demonstrating that cytosolic delivery GRx1 significantly rescued HT4 neural cells against GSSG or arachidonic acid-induced cytotoxicity (Fig. 9). These observations collectively support the notion that glutamate induces S-glutathionylation of 12-lipoxygenase in HT4 neural cells. GRx1 protected against glutamate-induced 12-lipoxygenase glutathionylation as well as cell death.

The estimated concentration of GSH in the brain is 1.9 ± 0.37 mM (13). Consistent with the literature (14), resting GSH levels in the mouse brain tissue was noted to be 2.8 μmol per gram wet weight (not shown). Acute ischemic stroke, as illustrated in Fig. 10A–B, resulted in over 7-fold increase in GSSG levels of the affected brain (Fig. 10C). We have previously reported that 12-lipoxygenase deficient mice are protected against brain injury caused by acute ischemic stroke (5). To test whether GSSG is indeed capable of causing brain lesion *in vivo*, GSSG was directly stereotaxically injected into the cortex. Evidence of clear infarction was noted (Fig. 10D). 12-Lipoxygenase deficient mice were significantly protected against GSSG-induced lesion of the cortex *in vivo* (Fig. 10E–F). These results indicate that under specific conditions GSSG may cause brain lesion *in vivo via* a 12-lipoxygenase dependent pathway.

Discussion

In mammals, the intracellular synthesis of glutathione and its utilization is described by the γ-glutamyl cycle, a concept that was put forth almost four decades ago (15). Reduced glutathione represents the centerpiece of the γ-glutamyl cycle, involved in several fundamental biological functions, including free radical scavenging, detoxification of

xenobiotics and carcinogens, redox reactions, biosynthesis of DNA, proteins and leukotrienes, as well as neurotransmission. While GSH may form numerous adducts in the human body (16), the most abundant GSH derivative is represented by GSSG. Oxidation of intracellular GSH by oxidants such as hydrogen peroxide and organic peroxides generally leads to the formation of GSSG. GSH can be further oxidized to the sulfenic, sulfinic, and sulfonic acid derivatives via successive two-electron oxidations of the thiol group.

GSSG is mostly viewed as a byproduct of GSH generated following reaction of GSH with an oxidizing species. As a result, GSSG/GSH ratio in the tissue emerged as a frequently used biochemical measure of oxidative stress (17). Advances in the concept of redox signaling, and redefining of oxidative stress in that light (18), has led to rethinking of the significance of GSSG in the cell (19). It is now widely acknowledged that changes in the cellular reduced/oxidized glutathione ratio trigger signal transduction mechanisms influencing cell survival. GSSG is capable of causing protein S-glutathionylation or reversible formation of protein mixed disulfides (protein-SSG). Post-translational reversible S-glutathionylation is known to regulate signal transduction as well as activities of several redox sensitive thiol-proteins (12).

Studies with exogenous non-permeable GSSG have demonstrated that extracellular GSSG may trigger apoptosis by a redox-mediated p38 mitogen-activated protein kinase pathway (20). While this addresses the significance of extracellular GSSG, the specific properties of intracellular GSSG remain under veil. GSH is oxidized to GSSG within the cell and pumped to the extracellular compartment (3, 4). Intracellular compartment being the primary site of GSSG generation, the significance of this disulfide within the cell becomes an important issue to address. Studies examining the significance of intracellular GSSG are complicated by the lack of a specific approach that would only elevate intracellular GSSG levels. For example, exposure of cells to pathogen related chemicals or to direct oxidant insult does elevate cellular GSSG but activates numerous other aspects of cell signaling (21). While the study of GSSG driven reactions in a cell-free system is relatively straightforward in approach, the *in vivo* significance of such findings remains questionable (22). This work presents first evidence from the use of a microinjection approach to study the significance of GSSG within the cell. Previously, we have utilized this approach to differentially study the cytosolic and nuclear compartments of HT4 cells as well as of primary cortical neurons (5). The approach is powerful in instantly and selectively introducing agents into specific compartments of the cell. Results of this study provide the first evidence demonstrating that the specific elevation of GSSG within the cell may cause cell death. Our observation demonstrating loss of mitochondrial membrane potential without affecting cell membrane integrity argues in favor of an apoptotic fate. Disorders of the central nervous system are frequently associated with concomitant glutathione depletion and oxidation (23, 24). Our observation that cells with compromised GSH levels are substantially more sensitive to GSSG-induced death leads to the notion that GSSG may play a role in cell death under conditions of disease and aging. We note that in GSH-sufficient cells (experimental) 0.5 mM GSSG is lethal. In GSH-deficient cells, a condition that mimics oxidative stress situation, the threshold of lethality sharply goes down by 20 fold to 0.025 mM GSSG. Our estimates show that in HT4 neural cells, total GSH content is in the range of 13 mM (not shown). This

is consistent with the literature reporting that under basal conditions, cellular GSH levels is in the tune of 10 mM (25, 26). In response to oxidant insult, GSSG levels sharply go up and may represent up to 50% of the total GSH in the cell (11, 27). Oxidative stress depletes cellular reducing equivalents such NADPH (28) compromising GSSG reductase function.

Glutamate toxicity is a major contributor to pathological cell death within the nervous system and is known to be mediated by reactive oxygen species and GSH loss (29, 30). Glutamate-induced death of neural cells is known to be associated with GSH loss and oxidation (6, 7). Our previous studies have identified 12-lipoxygenase as a key mediator of glutamate-induced neural cell death (5). We and others have reported that 12-lipoxygenase deficient mice are protected against stroke dependent injury to the brain (5, 31). GSH depletion causes neural degeneration by activating the 12-Lox pathway (32–34). Observations in this study suggest a direct influence of GSSG on 12-lipoxygenase activation. Arachidonic acid is converted into several more polar products in addition to 12-l-hydroperoxyeicosa-5,8,10,14-tetraenoic acid (12-HPETE) and 12-lhydroxyeicosa-5,8,10,14-tetraenoic acid (12-HETE) by 12-lipoxygenase. Previously it has been demonstrated that the presence of 0.5–1.5 mM GSH in the reaction mixture prevents the formation of the more polar products and produces 12-HETE as the only metabolite from arachidonic acid by the 12-lipoxygenase pathway. It was therefore concluded that 12-HPETE peroxidase in the 12-lipoxygenase pathway is a GSH-dependent peroxidase and the more polar products might be formed from the nonenzymatic breakdown of the primary 12-lipoxygenase product of 12-HPETE, owing to insufficient capability of the subsequent peroxidase system to completely reduce 12-HPETE to 12-HETE (35). In a cell system, disulfides are known to be able to act as biological oxidants that oxidize the zinc-thiolate clusters in metallothionein with concomitant zinc release (36). Intracellular zinc release is known to cause 12-lipoxygenase activation and neurotoxicity (37). Studies with BSO-treated GSH-deficient cells highlighted the significance of microinjected free arachidonic acid in neurotoxicity. These observations are consistent with the literature reporting a central role of the free arachidonic acid mobilizing enzyme phospholipase A2 in neurotoxicity (38).

S-Glutathionylated proteins (PSSG) can result from thiol/disulfide exchange between protein thiols (PSH) and GSSG (2). Protein S-glutathionylation, the reversible binding of glutathione to low-pKa cysteinyl residues in PSH, is involved in the redox regulation of protein function. Several enzymes are known to undergo this post translational modification. Importantly, whether glutathionylation inhibits or augments protein function may vary depending on the individual case. For example, glutathionylation inhibits phosphofructokinase (39), NFκB (40), glyceraldehydes-3-phosphate dehydrogenase (41), protein kinase C-α (42), creatine kinase (18), as well as actin (33). In contrast, glutathionylation-dependent gain of protein function has been reported for microsomal glutathione S-transferase (43), HIV-1 protease-Cys67 (44), and matrix metalloproteinases (45). Furthermore, specific electron transport proteins of the mitochondria are sensitive to S-glutathionylation (28, 46). Consistently, we noted that GSSG induced cell death was associated with loss of mitochondrial membrane potential. The presence of multiple cysteine residues in 12-lipoxygenase makes it susceptible to S-glutathionylation. Results of this study provide first evidence demonstrating that 12-lipoxygenase may be glutathionylated in glutamate challenged neural cells. The finding that both glutaredoxin-1 expression as well as

delivery may protect cells against glutamate-induced neurotoxicity suggests that glutamate-induced glutathionylation is implicated in the cell death pathway. GSSG is a functionally active byproduct of GSH metabolism that, under appropriate conditions, may trigger cell death. S-glutathionylation seems to be a mechanism that favors 12-lipoxygenase but not the classical caspase-3 dependent (47) death pathway.

The GSSG reductase inhibitor BCNU, clinically known as carmustine, is a proven chemotherapeutic agent (48). Cytotoxicity is a widely recognized side-effect of BCNU (49). Because BCNU treatment is associated with GSSG accumulation in cells (50), the significance of GSSG in BCNU-induced cytotoxicity is of interest. Observations of this study support that both GSSG as well as BCNU-induced cell death follow the same 12-lipoxygenase dependent path suggesting the possibility that BCNU may cause cell death *via* GSSG. Affirmation of this hypothesis would warrant examining the significance of pro-GSSG strategies for cancer therapy. Major forms of cancer therapy including radiation therapy as well as chemotherapy rely on oxygen-centered free radicals for their action. Thus, these interventions cause overt oxidative insult associated with elevated levels of cellular and tissue GSSG (51, 52). GSSG generated within the cell is pumped out of the cell perhaps to avert cytotoxicity caused by GSSG accumulation. Approaches to selectively block the GSSG efflux mechanisms in cancer cells might be useful for cancer therapy. Findings of this study support that BSO sensitizes cells to GSSG-induced death. Indeed, BSO has been founds to be an useful adjunct for both radiation (53) as well as chemotherapy (54). Also, inhibition of GSSG efflux by inhibition of MRP1 enhanced BCNU-induced cytoxicity suggesting that GSSG extrusion play a role in neural sensitivity to GSSG.

Three-fourth of all stroke in humans occur in distributions of the middle cerebral artery (55). Therefore, MCAO represents a common approach to study stroke in small as well as large animals (5, 56). Using a MCAO approach we were able to obtain just over 16% infarction of the ipsilateral hemisphere as assessed by MRI. Stroke caused 8-fold increased in GSSG levels in the affected brain tissue. This is consistent with the known incidence of oxidative stress in the stroke affected brain (57). Our observation that the stereotaxic injection of GSSG to the brain may cause lesion by a 12-lipoxygenase sensitive mechanism leads to question the significance of GSSG in numerous brain pathologies commonly associated with elevated levels of GSSG in the brain (58, 59).

Taken together, this work presents first evidence demonstrating that intracellular GSSG may trigger cell death. GSSG cytotoxicity is substantially enhanced under conditions of compromised cellular GSH levels as observed during a wide variety of disease conditions as well as aging (59, 60). BSO-assisted glutathione lowering approaches are known to be effective to facilitate both chemo- as well as radiation- therapies. Furthermore, BCNU-dependent arrest of GSSG reductase activity leads to elevation of cellular GSSG and has chemotherapeutic functions. Findings of this study lead to question the significance of GSSG in such processes. From the standpoint of novel therapeutic approaches, strategies directed at improving or arresting cellular GSSG clearance may be effective in minimizing oxidative stress related tissue injury or potentiating the killing of tumor cells, respectively.

Materials and Methods

Materials

The following materials were obtained from the source indicated. Ascorbic acid, arachidonic acid, L-glutamic acid monosodium salt, dimethyl sulfoxide, oxidized L-glutathione, reduced L-glutathione, 1,3-bis(2-chloroethyl)-1-nitrosourea (BCNU), L-buthionine-[S,R]-sulfoximine (Sigma); α-tocotrienol (90%, Carotech Inc.); 12-lipoxygenase from porcine leukocytes, MK-571, 5,6,7-trihydroxyflavone (BL-15; baicalein; Biomol Research Laboratories); tetramethylrhodamine methyl ester (TMRM), Qdot® 605 ITK™ streptavidin conjugate kit 2μM solution, dextran alexa fluor® 488, anti-V5 antibody, calcein acetoxymethyl ester, PLUS™ Reagent, lipofectamine™ LTX Reagent (Invitrogen); 12-lipoxygenase (murine leukocyte) polyclonal antiserum (Cayman chemical); anti-glutathione monoclonal antibody (ViroGen Corporation); V5 antibody affinity purified agarose immobilized conjugate (Bethyl Laboratories); goat anti-mouse glutaredoxin 1/GLRX1 antibody (R&D systems, Inc); glutaredoxin 1, glutaredoxin 1 antibody (Abcam); membrane potential assay kit (Molecular Devices Corp.).

For cell culture, Dulbecco's modified Eagle medium, fetal calf serum, and penicillin and streptomycin were purchased from Invitrogen Corporation, Carlsbad, CA. Culture dishes were obtained from Nunc, Denmark.

Cell culture

Mouse hippocampal HT4 neural cells were grown in Dulbecco's modified Eagle's medium supplemented with 10% fetal calf serum, 100 units/ml penicillin, and 100 μg/ml streptomycin at 37°C in humidified atmosphere of 95% air and 5% CO_2 as described previously (5–7). *Glutamate treatment.* Immediately before experiments, the culture medium was replaced with fresh medium supplemented with serum and antibiotics. Glutamate (10mM) was added to the medium as an aqueous solution. No change in the medium pH was observed in response to the addition of glutamate (5, 6). *L-Buthionine-sulfoximine(BSO) treatment.* Before experiments, the culture medium was replaced as described above, and freshly prepared BSO (50μM) in sterile PBS was added to the medium as described in relevant legends. 1,3-Bis(2-chloroethyl)-1-nitrosourea(BCNU) treatment. Before experiment, the culture medium was replaced as described above, and BCNU (50μM) prepared in ethanol was added to the medium. Respective controls were treated with an equal volume of ethanol. α-Tocotrienol (TCT) and 5,6,7,-trihydroxyflavone (BL-15) treatment. A stock solution of TCT was prepared in ethanol, and BL-15 was prepared in dimethyl sulfoxide (DMSO). Before experiments, culture medium was replaced with fresh medium supplemented with serum and antibiotics, and TCT (1μM) or BL-15 (2.5μM) was added to the culture dishes as described in relevant legends.

Microinjection

The mouse hippocampal HT4 cells (0.1×10^6 / plate) were grown on 35mm plates 24h before microinjection. As previously described (5), microinjection was performed using a micromanipulator Femtojet B 5247 and Injectman NI 2 (Eppendorf, Hamburg, Germany) with 80 hPa of pressure and 0.2 s duration. The compensation pressure during injection was

40 hPa. The glass micropipettes were made from GD-1 glass capillaries (Narishige, Japan) by using a Narishige PC-10 Puller with heater set at 52.7°C. Cells were injected with GSSG, GSH, sham (PBS) or reagents described in the relevant legends, and live and dead cells were counted at 24h after microinjection. Stock solutions of GSSG and GSH were freshly prepared in sterile PBS, and co-injected with QDot streptavidin conjugate with the emission maximum near 605nm (Invitrogen). QDot streptavidin conjugate was used as a fluorescent marker to localize the injection site. Microinjection is likely to result in higher localized concentration of GSSG and GSH compared to the concentration estimated based on overall cell volume. The use of burst of pressure (80 hPa over 0.2s) during microinjection, however, helps distribute the injected substance in the cytosol as visualized by the cytosolic distribution of Qdot following microinjection. Digital images were collected using a specialized phase contrast as well as a fluorescent Zeiss Axiovert 200M microscope suited for imaging cells grown in routine culture plates. The sample stage was maintained at 37°C, and the sample gas environment was maintained exactly as in the culture incubator.

Reduced (GSH) and oxidized (GSSG) glutathione assay

GSH and GSSG were detected simultaneously in HT4 cells and mice brain tissues using an HPLC coulometric electrode array detector (CoulArray Detector, model 5600 with 12 channels; ESA Inc., Chelmsford, MA, USA) as described in our laboratory previously (5, 61). The CoulArray detector employs multiple channels set at specific redox potentials. Data were collected using channels set at 600, 700, and 800mV. The samples were snap-frozen and stored in liquid nitrogen until HPLC assay. Sample preparation, composition of the mobile phase, and specification of the column used were as previously reported (6, 61).

Measurement of mitochondrial membrane potential (ψ)

Mitochondrial membrane ψ was measured using the fluorescent lipophilic cationic dye tetramethylrhodamine methyl ester (TMRM), which accumulates within mitochondria in a potential dependent manner (62). Following 24h of seeding, HT4 cells were injected with 500 attomole GSSG or sham (PBS). Dextran alexa fluor 488 was co-injected, and used as a fluorescent marker. After 2h incubation, cells were resuspended in Hanks' balanced salt solution and stained with 8nM TMRM and 0.5 μl/ml plasma membrane potential indicator (PMPI) for 30 min at 37°C in the dark. The cells were washed with PBS, and digital images of stained live cells were collected using a Zeiss Axiovert 200M microscope (5, 63, 64).

Cell viability

The viability of cells in culture was assessed by measuring leakage of lactate dehydrogenase (LDH) from cells into media 24h following glutamate treatment using an *in vitro* toxicology assay kit from Sigma Chemical Co. (St. Louis, MO, USA). The protocol has been described in detail in a previous report (65). In brief, LDH leakage was determined using the following equation : % total LDH leaked = (LDH activity in the cell culture medium / total LDH activity) × 100 (5). Total LDH activity represents the sum of LDH activities in the cell monolayer, detached cells, and the cell culture medium. Survival of HT4 cells was also quantified by using a calcein acetoxymethyl ester (AM) assay (10, 66, 67). Briefly, HT4 cells (40,000/well) were seeded in 12-well plates. After 2h of incubation, cells were treated

with either 2.5 μM BL-15 or 1μM TCT. After 6h incubation, cells were treated with 50μM BCNU. Following 12h incubation, media was removed from each well, and 5μM calcein AM in sterile PBS was added. After incubation at 37°C for 1h, fluorescence was measured by using the fluorescence multiwell plate reader Cyto Fluor™ II (PerSeptive Biosystems) with the excitation wavelength at 485nm and the emission wavelength of 530nm.

Determination of 12-lipoxygenase activity

The *in vitro* activity of 12-Lox was assayed using a standard spectrophotometric method measuring the increase in the formation of conjugated dienes from the substrate arachidonic acid as described (68), with minor modifications as specified below. To ensure greater solubility of arachidonic acid and to minimize the use of ethanol in the assay medium, the potassium salt of arachidonic acid was freshly prepared by mixing arachidonic acid with 0.1M KOH (1:1). The final assay mixture (total volume of 1ml) contained 10 μmol/L of arachidonic acid (10 μl from 1mmol/L stock) and 2 units of 12-Lox (porcine leukocyte enzyme) in 100 mmol/L Tris-HCl buffer (pH 7.4). The mixture was then gently mixed, reaction was started by adding the enzyme, and absorbance of the reaction mixture was measured at 234 nm (as an index of formation of conjugated dienes) using a Shimadzu model UV-2401PC spectrophotometer. The activity of 12-Lox was calculated from the absorbance values as n mole/min using the ε of 2.52×10^4 mol/L^{-1} and normalized as % control (5).

12-Lipoxygenase overexpression

This procedure was performed as described previously (5). Following 24h of seeding (0.5×10^6 / well), HT4 cells were transfected with plasmid pcDNA3.1 + 12-Lox (ResGen; Invitrogen) or empty pcDNA 3.1 containing V5 epitope tag using Lipofectamine™ LTX Reagent (Invitrogen). Cells were maintained in regular culture conditions for 48h to allow for protein expression, and cells or cell lysates were treated as described in the respective figure legends.

Immunoprecipitation and immunoblots

HT4 cells (0.5×10^6 / well) were seeded in 6-well plates for immunoprecipitation as previously described (5). Cells were transfected with pcDNA3.1 + 12-Lox or empty pcDNA 3.1 containing V5 epitope tag as described above. During harvest, the cells were washed with ice-cold phosphate-buffered saline (pH 7.4) and lysed with 0.2ml lysis buffer (Cell signaling Technology, Inc). Protein concentration was determined using the BCA protein assay kit (Pierce Biotechnology). Cells were treated as described in the respective figure legends, and then cell lysates (500μg) were incubated with 20μl immunoprecipitating antibody overnight at 4°C (V5 antibody affinity purified agarose immobilized conjugate, Bethyl Laboratories, Inc). Immunoprecipitated complexes were washed four times with lysis buffer (centrifugation at $1000 \times g$ at 4°C for 5 minutes), and boiled for 30 min under non-reducing conditions. Next, equal volumes of samples were loaded onto SDS-PAGE gel and probed with anti-V5 antibody (1: 5000 dilution, Invitrogen).

GSSG-induced glutathionylation

HT4 cell lysates (20μg) or 12-lipoxygenase from porcine leukocytes (30μg) were incubated with 10mM GSSG or the same volume of PBS at 37°C. After 1h incubation, samples were either processed for immunoprecipitation or subjected to SDS-PAGE under non-reducing conditions. Samples were quickly centrifuged, resuspended with sample buffer lacking thiol reductant, and boiled for 30min. After quick centrifugation, samples were loaded to 10% SDS-PAGE, and transferred to PVDF. After transfer, membranes were blocked using 10% nonfat milk overnight at 4 °C, and incubated with anti-glutathione monoclonal antibody (1:500 dilution, ViroGen Corporation), or anti-12-lipoxygenase polyclonal antibody (1:1000 dilution, Cayman chemical) for 2.5h. Membranes were washed three times. Next, blots were incubated with secondary antibody (1: 2000 dilution, Amersham anti-mouse IgG horseradish peroxidase linked whole antibody, GE Healthcare), or (1: 3000 dilution, Amersham anti-rabbit IgG horseradish peroxidase linked whole antibody, GE Healthcare) for 1 h, and visualized by enhanced chemiluminescence Western blotting detection reagent (GE Healthcare).

Adenoviral expression of glutaredoxin 1

The mouse hippocampal HT4 cells (0.5×10^6 / well) were grown on 6-well plates for 24 h, and infected with specific multiplicities of infection (m.o.i. 100, 200, 500, 1000, and 2000) of adenoviral vector containing the GRx1 cDNA construct (Ad-GRx1, a gift from Dr. J.J. Mieyal, Case Western Reserve University, Cleveland, OH, U.S.A.) or ad-LacZ (control) in 750 μl of serum-free DMEM for 4h. Cells were cultured for 72h in Dulbecco's modified Eagle's medium supplemented with 10% fetal calf serum, 100 units/ml penicillin, and 100 μg/ml streptomycin. Transfected cells or cell lysates were treated as described in relevant figure legends. After protein extraction, protein concentrations were determined using BCA protein reagents. Samples (30μg / lane) were separated on 12% SDS-PAGE and probed with anti-glutaredoxin 1 (1:1000 dilution, R&D systems, Inc). To evaluate the loading efficiency, membranes were re-probed with anti-GAPDH.

Immunocytochemistry

HT4 cells (0.5×10^6 / well) were seeded in 35mm plates for 24h, and transfected with ad-GRx1 as described above. Cells were washed with PBS three times and then fixed in 10% buffered formalin for 20 min. Next, the cells were washed three times with PBS followed by permeabilization using 0.1% Triton X-100/PBS for 15 min. The cells were washed three times with PBS and incubated with 10% goat serum (Vector Laboratories) for 1h at room temperature. Cells were then incubated with glutaredoxin-1 antibody (1:100, in 10% goat serum) overnight at 4°C. After incubation with primary antibody, cells were washed with PBS three times and incubated with an Alexa-flour rabbit (green) for 1h at room temperature. After three washes with PBS and incubation with 4',6'-diamino-2-phenylindole (1:10,000) for 2 min, cells were washed with PBS and mounted in gelmount (aqueous mount, Vector Laboratories) for microscopic imaging as described previously (5).

Stereotaxic injection

12-Lox knockout (B6.129S2-Alox15$^{tm/Fun}$) and corresponding background C57BL6/J mice were obtained from Jackson Laboratory. Young (8 to 10 week of age; 24–27g) male mice were anesthetized with isoflurane in oxygen-enriched air delivered through a facemask. The mouse was secured by ear bars, the skull was exposed, and injected with 5μl of GSSG stock (100 mM) in sterile PBS into the cortex using a Hamilton RN syringe with a stainless steel needle (Hamilton Company, Reno, Nevada). The location of injection site (coordinates: −0.5mm anterior, 3.5mm lateral, and 1.0mm ventral to bregma) was measured by Benchmark™ Stereotaxic Digital (myNeurolab.com, St.Louis, MO). To minimize pressure-induced damage, GSSG was injected at a rate of 0.2 μl/min. All animal protocols were approved by the Institutional Laboratory Animal Care and Use Committee (ILACUC) of the Ohio State University, Columbus, Ohio.

Mouse stroke model

Transient focal cerebral ischemia was induced in mice described above by middle cerebral artery (MCA) occlusion. Occlusion of the right middle cerebral artery was achieved by using the intraluminal filament insertion technique as previously described (5, 69, 70). Briefly, a 6-0 nylon monofilament was inserted into the internal carotid artery, *via* the external carotid artery. Then the filament tip was positioned for occlusion at a distance of 6mm beyond the internal carotid artery-pterygopalatine artery bifurcation. We observed that this approach results in a 60% to 70% drop in cerebral blood flow as measured by laser Doppler (DRT4, Moor Instruments). Once the filament was secured, the incision was sutured and the animal was allowed to recover from anesthesia in its home cage. After 90 min of occlusion, the animal was briefly re-anesthetized, and reperfusion was initiated via withdrawal of the filament. This surgical protocol typically results in a core infarct limited to the parietal cerebral cortex and caudate putamen of the right hemisphere. After 24h of reperfusion, a T2-weighted image was taken to measure infarct volume, and left and right hemispheres were collected in liquid nitrogen for GSH and GSSG measurements.

Magnetic resonance imaging (MRI)

T2-weighted imaging was performed on stereotaxically-injected as well as stroke-affected mice. Imaging experiments were carried out in an 11.7T (500 MHz) MR system comprised of a vertical bore magnet (Bruker Biospin, Ettlingen, Germany) as described previously by our group (71). High-resolution magnetic resonance imaging was performed on mice brain. Mice were anesthetized by inhaled isoflurane *via* a nose cone. The mouse under MR scan was placed in a MR compatible animal holder with the proper respiratory sensor unit. The mouse was held with tape during contingent supply of a mixture of carboxin (95% air and 5% carbon dioxide) and isoflurane through tubing. A 30 mm birdcage coil was used which surrounds the mouse brain. The animal was then placed inside the radio frequency coil (resonator) and finally the whole arrangement was placed inside the vertical magnet. A spin echo (SE) sequence was used to acquire T2-weighted MR images from the mouse head on the 11.7-T MRI system. A spin echo technique with rapid acquisition with relaxation enhancement (RARE) sequence providing 8 echo train length (ETL) was used with the following parameters: field of view (FOV) = 30×30 mm, acquisition matrix 256×256,

repetition time (TR) = 3000 ms, echo time (TE) = 30 ms, flip angle (FA) = 180 degrees, images in acquisition = 15, resolution = 8.533 pixels/mm, and number of averages 4. Shim currents were initialized by manual adjustments on all linear and higher order field inhomogeneities. After several localizer scans were completed, a T2-weighted spin echo RARE sequence was applied to generate 15 images corresponding to 15 short axis slices. Post image processing was done using ImageJ software (NIH). For stroke-volume calculation from 2D images, raw MRI images were first converted to digital imaging and communications in medicine (DICOM) format and read into ImageJ software. By delineating both the whole brain and injured part of the brain borders, whole brain area and injury area were calculated. The areas were summed from all short axis slices and the volumes were computed from the area of traced boarders by multiplying slice thickness. A percentage fraction of infarction to whole brain was determined from the volumes calculated as above.

Statistical analyses

Data are reported as mean ± S.D. of at least three experiments. Difference between two means was tested by Student *t* test. Comparisons between multiple groups were made by analysis of variance. p<0.05 was considered statistically significant.

Supplementary Material

Refer to Web version on PubMed Central for supplementary material.

Acknowledgements

Abbreviations list

12-Lox	12-lipoxygenase
BCNU	1,3-bis(2-chloroethyl)-1-nitrosourea
BL-15	5,6,7,-trihydroxyflavone
BSO	L-buthioninesulfoximine
GRx1	glutaredoxin-1
GSH	reduced glutathione
GSSG	glutathione disulfide
LDH	lactate dehydrogenase
MCA	middle cerebral artery
PMPI	plasma membrane potential indicator
TCT	α-tocotrienol
TMRM	tetramethylrhodamine methyl ester

References

1. Lenton KJ, Therriault H, Wagner JR. Analysis of glutathione and glutathione disulfide in whole cells and mitochondria by postcolumn derivatization high-performance liquid chromatography with ortho-phthalaldehyde. Anal Biochem. 1999; 274(1):125–30. [PubMed: 10527505]

2. Rossi R, Dalle-Donne I, Milzani A, Giustarini D. Oxidized forms of glutathione in peripheral blood as biomarkers of oxidative stress. Clin Chem. 2006; 52(7):1406–14. [PubMed: 16690733]

3. Sen CK, Rahkila P, Hanninen O. Glutathione metabolism in skeletal muscle derived cells of the L6 line. Acta Physiol Scand. 1993; 148(1):21–6. [PubMed: 8333293]

4. Srivastava SK, Beutler E. The transport of oxidized glutathione from human erythrocytes. J Biol Chem. 1969; 244(1):9–16. [PubMed: 5773294]

5. Khanna P, Nehru B. Antioxidant enzymatic system in neuronal and glial cells enriched fractions of rat brain after aluminum exposure. Cell Mol Neurobiol. 2007; 27(7):959–69. [PubMed: 18041579]

6. Sen CK, Khanna S, Roy S, Packer L. Molecular basis of vitamin E action. Tocotrienol potently inhibits glutamate-induced pp60(c-Src) kinase activation and death of HT4 neuronal cells. J Biol Chem. 2000; 275(17):13049–55. [PubMed: 10777609]

7. Tirosh O, Sen CK, Roy S, Packer L. Cellular and mitochondrial changes in glutamate-induced HT4 neuronal cell death. Neuroscience. 2000; 97(3):531–41. [PubMed: 10828535]

8. Galter D, Mihm S, Droge W. Distinct effects of glutathione disulphide on the nuclear transcription factor kappa B and the activator protein-1. Eur J Biochem. 1994; 221(2):639–48. [PubMed: 8174544]

9. Haddad JJ, Safieh-Garabedian B, Saade NE, Lauterbach R. Inhibition of glutathione-related enzymes augments LPS-mediated cytokine biosynthesis: involvement of an IkappaB/NF-kappaB-sensitive pathway in the alveolar epithelium. Int Immunopharmacol. 2002; 2(11):1567–83. [PubMed: 12433058]

10. Hirrlinger J, Konig J, Keppler D, Lindenau J, Schulz JB, Dringen R. The multidrug resistance protein MRP1 mediates the release of glutathione disulfide from rat astrocytes during oxidative stress. J Neurochem. 2001; 76(2):627–36. [PubMed: 11208926]

11. Minich T, Riemer J, Schulz JB, Wielinga P, Wijnholds J, Dringen R. The multidrug resistance protein 1 (Mrp1), but not Mrp5, mediates export of glutathione and glutathione disulfide from brain astrocytes. J Neurochem. 2006; 97(2):373–84. [PubMed: 16539673]

12. Mieyal JJ, Gallogly MM, Qanungo S, Sabens EA, Shelton MD. Molecular mechanisms and clinical implications of reversible protein s-glutathionylation. Antioxid Redox Signal. 2008; 10(11):1941–88. [PubMed: 18774901]

13. Satoh T, Yoshioka Y. Contribution of reduced and oxidized glutathione to signals detected by magnetic resonance spectroscopy as indicators of local brain redox state. Neurosci Res. 2006; 55(1):34–9. [PubMed: 16503064]

14. Ghizoni DM, Pavanati KC, Arent AM, Machado C, Faria MS, Pinto CM, Gasparotto OC, Goncalves S, Dafre AL. Alterations in glutathione levels of brain structures caused by acute restraint stress and by nitric oxide synthase inhibition but not by intraspecific agonistic interaction. Behav Brain Res. 2006; 166(1):71–7. [PubMed: 16140401]

15. Orlowski M, Meister A. The gamma-glutamyl cycle: a possible transport system for amino acids. Proc Natl Acad Sci U S A. 1970; 67(3):1248–55. [PubMed: 5274454]

16. Blair IA. Endogenous glutathione adducts. Curr Drug Metab. 2006; 7(8):853–72. [PubMed: 17168687]

17. Schafer FQ, Buettner GR. Redox environment of the cell as viewed through the redox state of the glutathione disulfide/glutathione couple. Free Radic Biol Med. 2001; 30(11):1191–212. [PubMed: 11368918]

18. Reddy S, Jones AD, Cross CE, Wong PS, Van Der Vliet A. Inactivation of creatine kinase by S-glutathionylation of the active-site cysteine residue. Biochem J. 2000; 347(Pt 3):821–7. [PubMed: 10769188]

19. Circu ML, Aw TY. Glutathione and apoptosis. Free Radic Res. 2008; 42(8):689–706. [PubMed: 18671159]

20. Filomeni G, Rotilio G, Ciriolo MR. Glutathione disulfide induces apoptosis in U937 cells by a redox-mediated p38 MAP kinase pathway. Faseb J. 2003; 17(1):64–6. [PubMed: 12424221]

21. Kirsch JD, Yi AK, Spitz DR, Krieg AM. Accumulation of glutathione disulfide mediates NF-kappaB activation during immune stimulation with CpG DNA. Antisense Nucleic Acid Drug Dev. 2002; 12(5):327–40. [PubMed: 12477282]

22. den Hartog GJ, Haenen GR, Vegt E, van der Vijgh WJ, Bast A. Efficacy of HOCl scavenging by sulfur-containing compounds: antioxidant activity of glutathione disulfide? Biol Chem. 2002; 383(3–4):709–13. [PubMed: 12033460]

23. Dringen R, Hirrlinger J. Glutathione pathways in the brain. Biol Chem. 2003; 384(4):505–16. [PubMed: 12751781]

24. Schulz JB, Lindenau J, Seyfried J, Dichgans J. Glutathione, oxidative stress and neurodegeneration. Eur J Biochem. 2000; 267(16):4904–11. [PubMed: 10931172]

25. Meister A, Anderson ME. Glutathione. Annu Rev Biochem. 1983; 52:711–60. [PubMed: 6137189]

26. Shaw, CA. Glutathione in the nervous system. Taylor & Francis; Washington, DC: 1998. p. xivp. 389

27. Pias EK, Aw TY. Early redox imbalance mediates hydroperoxide-induced apoptosis in mitotic competent undifferentiated PC-12 cells. Cell Death Differ. 2002; 9(9):1007–16. [PubMed: 12181751]

28. Cheng W, Fu YX, Porres JM, Ross DA, Lei XG. Selenium-dependent cellular glutathione peroxidase protects mice against a pro-oxidant-induced oxidation of NADPH, NADH, lipids, and protein. Faseb J. 1999; 13(11):1467–75. [PubMed: 10428770]

29. Coyle JT, Puttfarcken P. Oxidative stress, glutamate, and neurodegenerative disorders. Science. 1993; 262(5134):689–95. [PubMed: 7901908]

30. Herrera F, Martin V, Garcia-Santos G, Rodriguez-Blanco J, Antolin I, Rodriguez C. Melatonin prevents glutamate-induced oxytosis in the HT22 mouse hippocampal cell line through an antioxidant effect specifically targeting mitochondria. J Neurochem. 2007; 100(3):736–46. [PubMed: 17263795]

31. van Leyen K, Kim HY, Lee SR, Jin G, Arai K, Lo EH. Baicalein and 12/15-lipoxygenase in the ischemic brain. Stroke. 2006; 37(12):3014–8. [PubMed: 17053180]

32. Canals S, Casarejos MJ, de Bernardo S, Rodriguez-Martin E, Mena MA. Nitric oxide triggers the toxicity due to glutathione depletion in midbrain cultures through 12-lipoxygenase. J Biol Chem. 2003; 278(24):21542–9. [PubMed: 12679339]

33. Hwang C, Sinskey AJ, Lodish HF. Oxidized redox state of glutathione in the endoplasmic reticulum. Science. 1992; 257(5076):1496–502. [PubMed: 1523409]

34. Li Y, Maher P, Schubert D. A role for 12-lipoxygenase in nerve cell death caused by glutathione depletion. Neuron. 1997; 19(2):453–63. [PubMed: 9292733]

35. Chang WC, Nakao J, Orimo H, Murota S. Effects of reduced glutathione on the 12-lipoxygenase pathways in rat platelets. Biochem J. 1982; 202(3):771–6. [PubMed: 6807297]

36. Maret W. Cellular zinc and redox states converge in the metallothionein/thionein pair. J Nutr. 2003; 133(5 Suppl 1):1460S–2S. [PubMed: 12730443]

37. Wang H, Li J, Follett PL, Zhang Y, Cotanche DA, Jensen FE, Volpe JJ, Rosenberg PA. 12-Lipoxygenase plays a key role in cell death caused by glutathione depletion and arachidonic acid in rat oligodendrocytes. Eur J Neurosci. 2004; 20(8):2049–58. [PubMed: 15450084]

38. Muralikrishna Adibhatla R, Hatcher JF. Phospholipase A2, reactive oxygen species, and lipid peroxidation in cerebral ischemia. Free Radic Biol Med. 2006; 40(3):376–87. [PubMed: 16443152]

39. Mieyal JJ, Starke DW, Gravina SA, Dothey C, Chung JS. Thioltransferase in human red blood cells: purification and properties. Biochemistry. 1991; 30(25):6088–97. [PubMed: 1829380]

40. Pineda-Molina E, Klatt P, Vazquez J, Marina A, Garcia de Lacoba M, Perez-Sala D, Lamas S. Glutathionylation of the p50 subunit of NF-kappaB: a mechanism for redox-induced inhibition of DNA binding. Biochemistry. 2001; 40(47):14134–42. [PubMed: 11714266]

41. Mohr S, Hallak H, de Boitte A, Lapetina EG, Brune B. Nitric oxide-induced S-glutathionylation and inactivation of glyceraldehyde-3-phosphate dehydrogenase. J Biol Chem. 1999; 274(14): 9427–30. [PubMed: 10092623]

42. Ward NE, Stewart JR, Ioannides CG, O'Brian CA. Oxidant-induced S-glutathiolation inactivates protein kinase C-alpha (PKC-alpha): a potential mechanism of PKC isozyme regulation. Biochemistry. 2000; 39(33):10319–29. [PubMed: 10956021]

43. Dafre AL, Sies H, Akerboom T. Protein S-thiolation and regulation of microsomal glutathione transferase activity by the glutathione redox couple. Arch Biochem Biophys. 1996; 332(2):288–94. [PubMed: 8806737]

44. Davis DA, Newcomb FM, Starke DW, Ott DE, Mieyal JJ, Yarchoan R. Thioltransferase (glutaredoxin) is detected within HIV-1 and can regulate the activity of glutathionylated HIV-1 protease in vitro. J Biol Chem. 1997; 272(41):25935–40. [PubMed: 9325327]

45. Okamoto T, Akaike T, Sawa T, Miyamoto Y, van der Vliet A, Maeda H. Activation of matrix metalloproteinases by peroxynitrite-induced protein S-glutathiolation via disulfide S-oxide formation. J Biol Chem. 2001; 276(31):29596–602. [PubMed: 11395496]

46. Hurd TR, Costa NJ, Dahm CC, Beer SM, Brown SE, Filipovska A, Murphy MP. Glutathionylation of mitochondrial proteins. Antioxid Redox Signal. 2005; 7(7–8):999–1010. [PubMed: 15998254]

47. Huang Z, Pinto JT, Deng H, Richie JP Jr. Inhibition of caspase-3 activity and activation by protein glutathionylation. Biochem Pharmacol. 2008; 75(11):2234–44. [PubMed: 18395187]

48. Chang SM, Prados MD, Yung WK, Fine H, Junck L, Greenberg H, Robins HI, Mehta M, Fink KL, Jaeckle KA, Kuhn J, Hess K, Schold C. Phase II study of neoadjuvant 1, 3-bis (2-chloroethyl)-1-nitrosourea and temozolomide for newly diagnosed anaplastic glioma: a North American Brain Tumor Consortium Trial. Cancer. 2004; 100(8):1712–6. [PubMed: 15073861]

49. Doroshenko N, Doroshenko P. Ion dependence of cytotoxicity of carmustine against PC12 cells. Eur J Pharmacol. 2003; 476(3):185–91. [PubMed: 12969765]

50. Smith AC, Boyd MR. Preferential effects of 1,3-bis(2-chloroethyl)-1-nitrosourea (BCNU) on pulmonary glutathione reductase and glutathione/glutathione disulfide ratios: possible implications for lung toxicity. J Pharmacol Exp Ther. 1984; 229(3):658–63. [PubMed: 6726651]

51. Navarro J, Obrador E, Pellicer JA, Aseni M, Vina J, Estrela JM. Blood glutathione as an index of radiation-induced oxidative stress in mice and humans. Free Radic Biol Med. 1997; 22(7):1203–9. [PubMed: 9098094]

52. Mkoji GM, Smith JM, Prichard RK. Glutathione redox state, lipid peroxide levels, and activities of glutathione enzymes in oltipraz-treated adult Schistosoma mansoni. Biochem Pharmacol. 1989; 38(23):4307–13. [PubMed: 2512935]

53. Leung SW, Mitchell JB, al-Nabulsi I, Friedman N, Newsome J, Belldegrun A, Kasid U. Effect of L-buthionine sulfoximine on the radiation response of human renal carcinoma cell lines. Cancer. 1993; 71(7):2276–85. [PubMed: 8095848]

54. Mistry P, Harrap KR. Historical aspects of glutathione and cancer chemotherapy. Pharmacol Ther. 1991; 49(1–2):125–32. [PubMed: 1852785]

55. Castillo, M. Neuroradiology companion: methods, guidelines and imaging fundamentals. Lippincott Williams & Wilkins; Philadelphia: 2006.

56. Khanna S, Roy S, Slivka A, Craft TK, Chaki S, Rink C, Notestine MA, DeVries AC, Parinandi NL, Sen CK. Neuroprotective properties of the natural vitamin E alpha-tocotrienol. Stroke. 2005; 36(10):2258–64. [PubMed: 16166580]

57. Cherubini A, Ruggiero C, Polidori MC, Mecocci P. Potential markers of oxidative stress in stroke. Free Radic Biol Med. 2005; 39(7):841–52. [PubMed: 16140205]

58. Hiramatsu M, Mori A. Reduced and oxidized glutathione in brain and convulsions. Neurochem Res. 1981; 6(3):301–6. [PubMed: 7279107]

59. Adams JD Jr. Klaidman LK, Odunze IN, Shen HC, Miller CA. Alzheimer's and Parkinson's disease. Brain levels of glutathione, glutathione disulfide, and vitamin E. Mol Chem Neuropathol. 1991; 14(3):213–26. [PubMed: 1958264]

60. Maher P. The effects of stress and aging on glutathione metabolism. Ageing Res Rev. 2005; 4(2): 288–314. [PubMed: 15936251]

61. Sen CK, Khanna S, Babior BM, Hunt TK, Ellison EC, Roy S. Oxidant-induced vascular endothelial growth factor expression in human keratinocytes and cutaneous wound healing. J Biol Chem. 2002; 277(36):33284–90. [PubMed: 12068011]

62. Reid AB, Kurten RC, McCullough SS, Brock RW, Hinson JA. Mechanisms of acetaminophen-induced hepatotoxicity: role of oxidative stress and mitochondrial permeability transition in freshly isolated mouse hepatocytes. J Pharmacol Exp Ther. 2005; 312(2):509–16. [PubMed: 15466245]

63. Duchen MR, Surin A, Jacobson J. Imaging mitochondrial function in intact cells. Methods Enzymol. 2003; 361:353–89. [PubMed: 12624920]

64. Nicholls DG. Simultaneous monitoring of ionophore- and inhibitor-mediated plasma and mitochondrial membrane potential changes in cultured neurons. J Biol Chem. 2006; 281(21):14864–74. [PubMed: 16551630]

65. Han D, Sen CK, Roy S, Kobayashi MS, Tritschler HJ, Packer L. Protection against glutamate-induced cytotoxicity in C6 glial cells by thiol antioxidants. Am J Physiol. 1997; 273(5 Pt 2):R1771–8. [PubMed: 9374822]

66. De Clerck LS, Bridts CH, Mertens AM, Moens MM, Stevens WJ. Use of fluorescent dyes in the determination of adherence of human leucocytes to endothelial cells and the effect of fluorochromes on cellular function. J Immunol Methods. 1994; 172(1):115–24. [PubMed: 8207260]

67. Van Damme P, Van Hoecke A, Lambrechts D, Vanacker P, Bogaert E, van Swieten J, Carmeliet P, Van Den Bosch L, Robberecht W. Progranulin functions as a neurotrophic factor to regulate neurite outgrowth and enhance neuronal survival. J Cell Biol. 2008; 181(1):37–41. [PubMed: 18378771]

68. Beierschmitt WP, McNeish JD, Griffiths RJ, Nagahisa A, Nakane M, Amacher DE. Induction of hepatic microsomal drug-metabolizing enzymes by inhibitors of 5-lipoxygenase (5-LO): studies in rats and 5-LO knockout mice. Toxicol Sci. 2001; 63(1):15–21. [PubMed: 11509739]

69. DeVries AC, Joh HD, Bernard O, Hattori K, Hurn PD, Traystman RJ, Alkayed NJ. Social stress exacerbates stroke outcome by suppressing Bcl-2 expression. Proc Natl Acad Sci U S A. 2001; 98(20):11824–8. [PubMed: 11553785]

70. Li X, Blizzard KK, Zeng Z, DeVries AC, Hurn PD, McCullough LD. Chronic behavioral testing after focal ischemia in the mouse: functional recovery and the effects of gender. Exp Neurol. 2004; 187(1):94–104. [PubMed: 15081592]

71. Ojha N, Roy S, Radtke J, Simonetti O, Gnyawali S, Zweier JL, Kuppusamy P, Sen CK. Characterization of the structural and functional changes in the myocardium following focal ischemia-reperfusion injury. Am J Physiol Heart Circ Physiol. 2008; 294(6):H2435–43. [PubMed: 18375718]
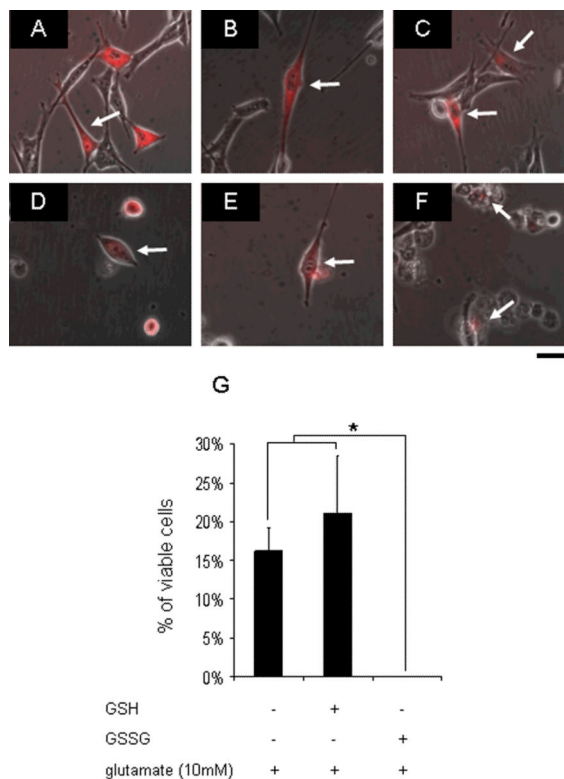
Figure 1. Microinjected GSH failed to rescue, while GSSG potentiated glutamate-induced death of HT4 neural cells

PBS (**A**), 500 attomole GSH (**B**), or GSSG (**C**) was injected into the cytoplasm after 4h glutamate challenge. After 24h incubation, some (15–20%) HT4 cells injected with PBS (**D**) or GSH (**E**) remained alive, while all GSSG (**F**) injected cells were dead (**G**) suggesting GSSG toxicity. attomoles injected [micromolar]i, n=3, Bar, 20 μm. *, lower than control. Results are mean ± S.D. *, $p < 0.05$.
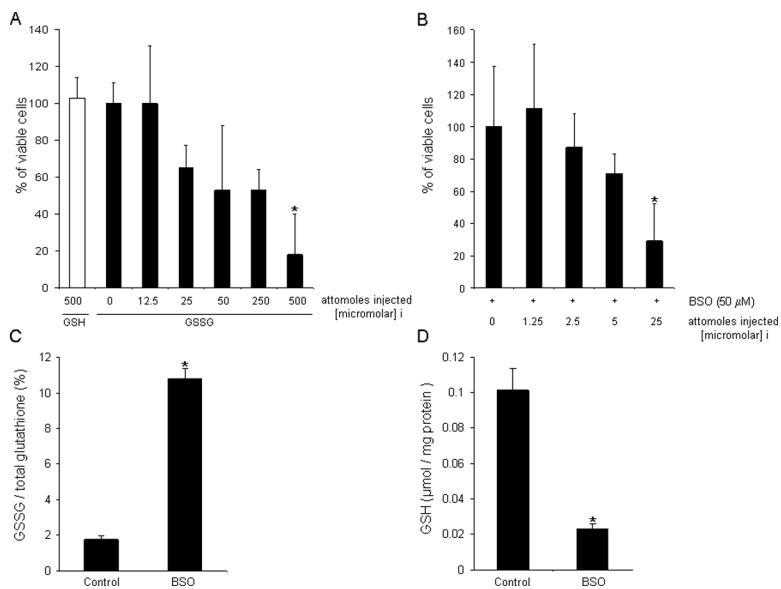
Figure 2. Dose dependent GSSG toxicity
A, 500 attomole GSH or GSSG (0, 12.5, 25, 50, 250, and 500 attomoles) was microinjected into the cytoplasm of HT4 cells for 24h. **B**, GSSG (0, 1.25, 2.5, 5 and 25 attomoles) was injected into the cytoplasm of HT4 cells pre-treated with 50 μM BSO for 12h. Cellular GSSG/total glutathione (**C**) was increased, and absolute value of GSH (μmol/ mg protein) was decreased after 50 μM BSO treatment (**D**). attomoles injected [micromolar]i, n=3, Results are mean ± S.D. *, $p < 0.05$.
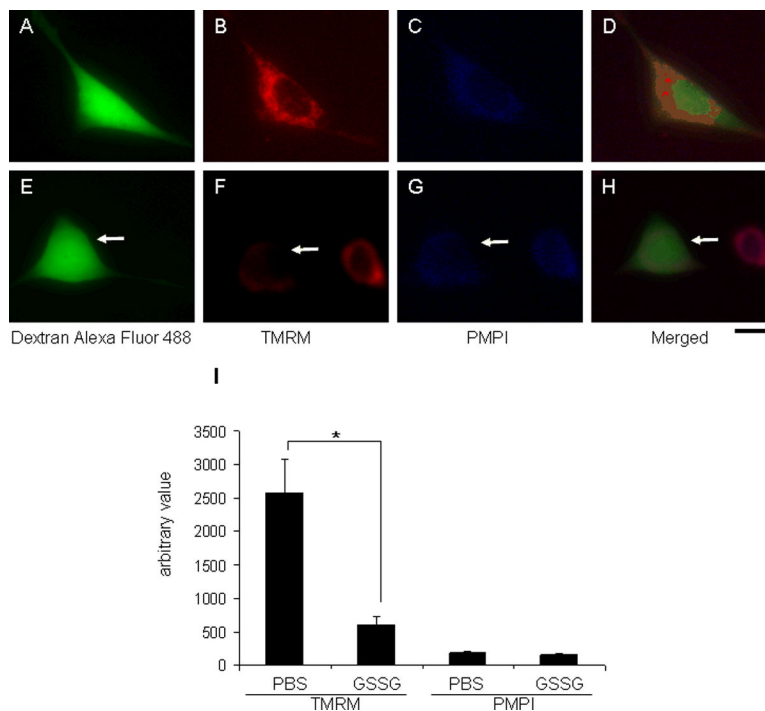
Figure 3. Cytosolic injection of GSSG compromised mitochondrial membrane potential
HT4 cells were injected with either PBS (**A**, Dextran alexa fluor 488; **B**, 8nM TMRM; **C**, 0.5 μl/ml PMPI; **D**, merged image) or 500 attomole GSSG (**E**, Dextran alexa fluor 488; **F**, 8nM TMRM; **G**, 0.5 μl/ml PMPI; **H**, merged image). Dextran alexa fluor 488 was co-injected to visualize injected cells. After 2h incubation, 8nM TMRM and 0.5 μl/ml PMPI were treated to cell culture medium. **I**, GSSG injected cells showed lower mitochondrial membrane potential (**F**) compared to sham injected cells (**B**) while plasma membrane potential was not affected (**C** and **G**). attomoles injected [micromolar]i, n=3, Bar, 30 μm. Results are mean ± S.D. *, $p < 0.05$.
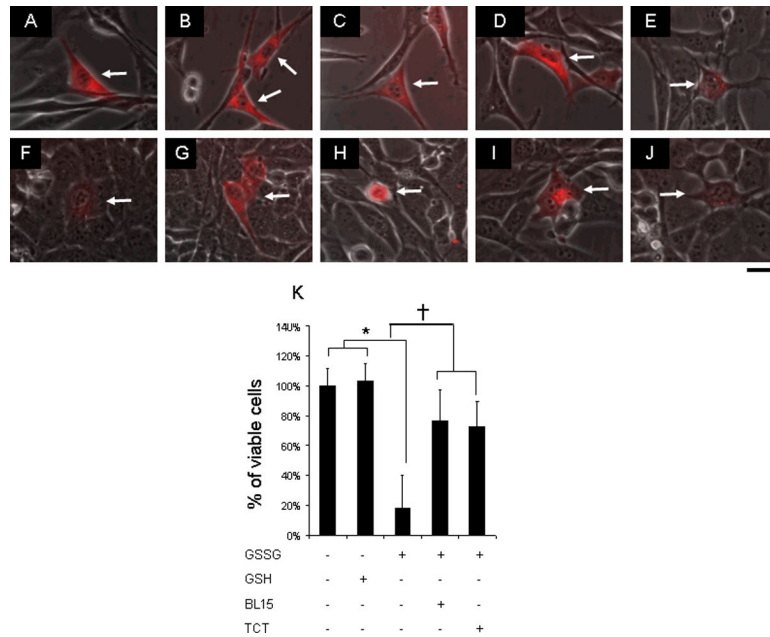
Figure 4. GSSG-induced cell death was attenuated by 12-lipoxygenase inhibitors
Cultured HT4 cells were injected with PBS (**A**), 500 attomole GSH (**B**), or 500 attomole GSSG (**C** to **E**). 2.5 μM BL-15 (**D**) and 1 μM TCT (**E**) were treated to culture medium prior to cytoplasmic injection with GSSG. After 24h incubation, cells injected with PBS (**F**) and GSH (**G**) were alive, while GSSG (**H**) injected cells were dead. Treatment of BL-15 (**I**) and TCT (**J**) protected neural cells against GSSG challenge (**K**). attomoles injected [micromolar]i, n=3, Bar, 20 μm. *, lower than control. †, higher than cells injected with GSSG. Results are mean ± S.D. *, $p < 0.05$.
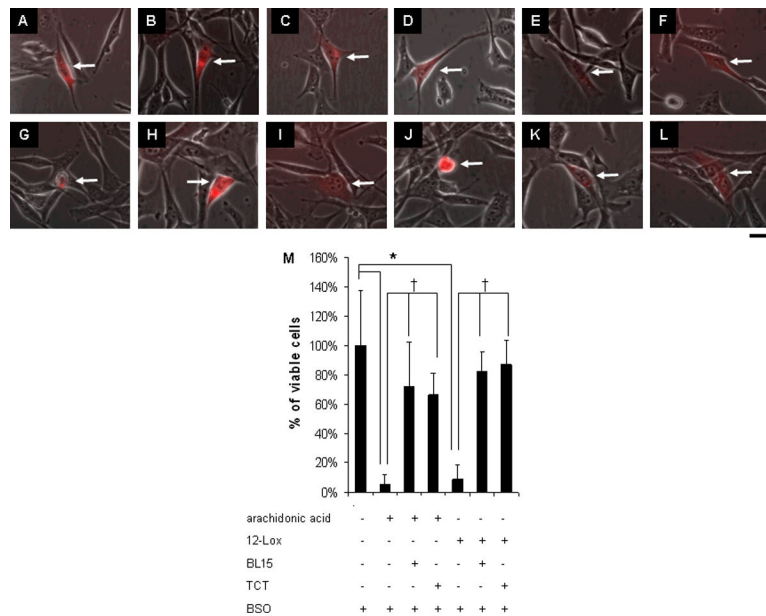
Figure 5. Arachidonic acid or 12-lipoxygenase induced cell death was attenuated by 12-lipoxygenase inhibitors

Cultured HT4 cells were treated with 50 μM BSO for 12h (**A** to **L**), and either 0.15 attomole arachidonic acid (**A, B**, and **C**) or 5×10^{-8} units 12-Lox (**D, E**, and **F**) were injected (marked by arrow) into cytoplasm (**A** and **D,** without treatment; **B** and **E**, 2.5 μM BL-15 added to culture medium prior to microinjection; **C** and **F**, 1 μM TCT added to culture medium prior to microinjection). After 24h incubation, cells injected with arachidonic acid (**G**) lost cell viability, while BL-15 (**H**) or TCT (**I**) treated cells were protected, and cells injected with 12-Lox (**J**) lost cell viability, while BL-15 (**K**) and TCT (**L**) treated cells were protected (**M**). attomoles injected [micromolar]i, n=3, Bar, 20 μm. *, lower than control, †, higher than cells without treatment of 12 Lox inhibitors. Results are mean ± S.D. *, $p < 0.05$.
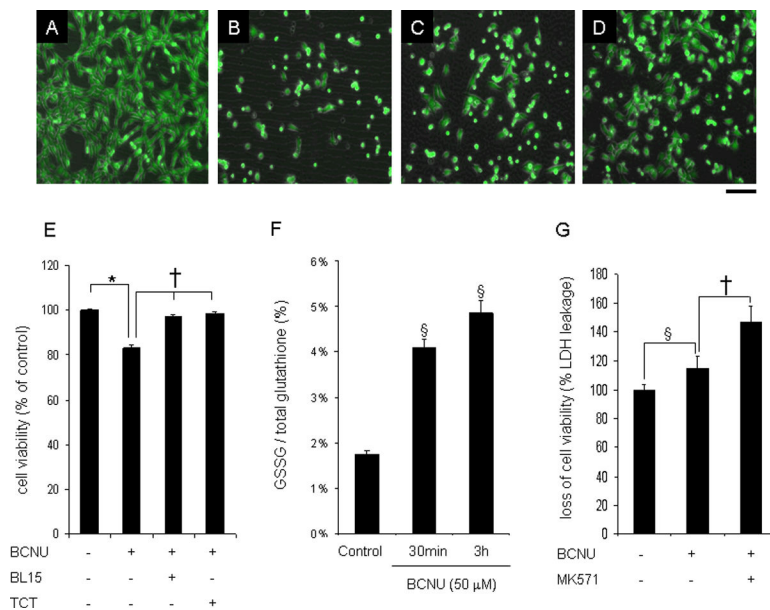
Figure 6. Bischloroethylnitrosourea induced cell death was attenuated by 12-lipoxygenase inhibitors

HT4 cells were treated with ethanol (**A**), 50 μM 1,3-Bis (2-chloroethyl)-1-nitrosourea; BCNU (**B**), 50 μM BCNU and 2.5 μM BL-15 (**C**), or 50 μM BCNU and 1 μM TCT (**D**). After 12h of BCNU treatment, live cells were visualized using calcein-AM (**A–D**); cell viability was also assayed using a calcein AM based cell viability kit (**E**). Cells treated with BL-15 or TCT were more resistant to BCNU-induced loss of cell viability. BCNU treatment increased cellular GSSG over time (**F**). **G**, MK571 (20μM) was added to HT4 cell culture medium for 6h prior to 50 μM BCNU treatment. After 12h of adding BCNU into cell culture medium, loss of cell viability was assessed by measuring leakage of lactate dehydrogenase (LDH). MK571 treated HT4 cells were more vulnerable to BCNU-induced loss of cell viability. n=3, Bar, 100 μm. *, lower than control, †, higher than BCNU-challenged HT4 cells, §, higher than control. Results are mean ± S.D. *, $p < 0.05$.
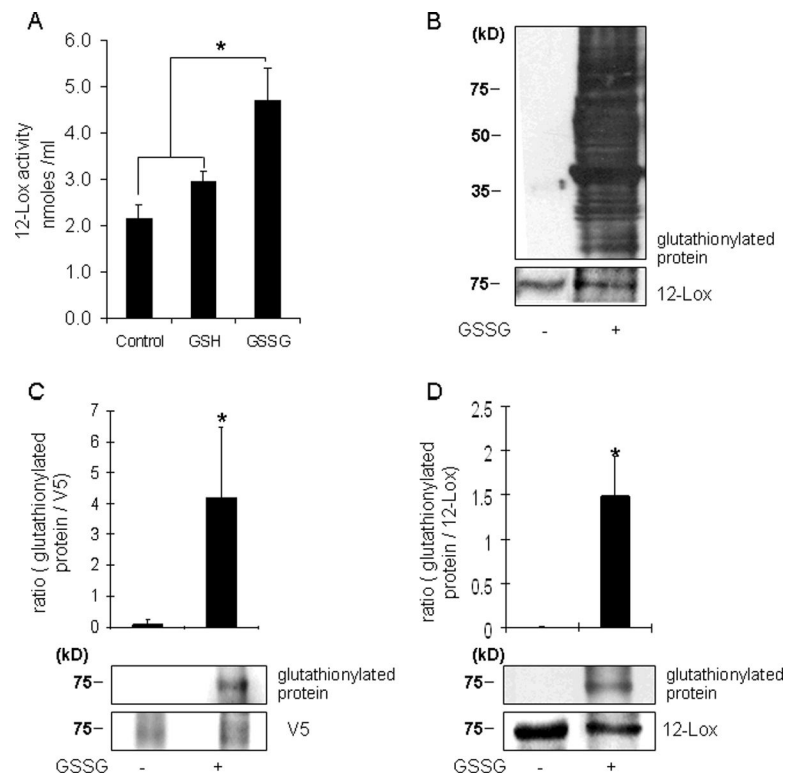
Figure 7. 12-Lipoxygenase activity and GSS-12-lipoxygenase formation in response to GSSG
A, The *in vitro* activity of 12-Lox was assayed by using a standard spectrophotometric method. The final assay mixture contained 10 μmol/L of arachidonic acid and 2 units of 12-Lox. To determine the effects of GSSG, 10 μM GSSG or GSH were incubated with this mixture as shown. The absorbance of the reaction mixture was measured at 234 nm as an index of formation of conjugated dienes. GSSG increased 12-Lox activity by increasing conjugated diene (reaction product) formation. **B**, HT4 cell lysates (20μg) were incubated with GSSG (10 mM) for 1h and subjected to SDS-PAGE and immunoblotting for the detection of formation of protein-glutathione mixed disulfides (glutathionylation). Cells incubated with GSSG were rich in glutathionylated proteins. **C**, After transfection with 12-Lox containing V5 epitope, HT4 cell lysates were incubated with 10mM GSSG for 1h and cell lysates (500μg) were subjected to immunoprecipitation (IP) with V5 antibody. IP were subjected to SDS-PAGE and immunoblotting for the detection of formation of protein-glutathione mixed disulfides. Cell lysates incubated with GSSG increased the formation of GSS-12-Lox. **D**, Porcine leukocytes 12-Lox (30μg) was incubated with 10mM GSSG for 1h. Western blot was used for detection of GSS-12-Lox formation. 12-Lox incubated with GSSG increased formation of glutathionylation. n=3, Results are mean ± S.D. *, $p < 0.05$.
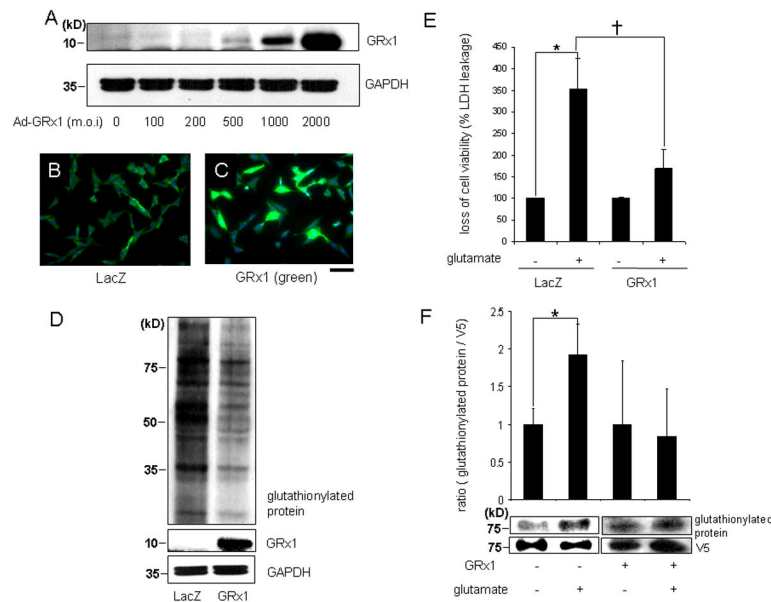
Figure 8. Glutaredoxin-1 reversed glutathionylation in HT4 neural cells and protected cells against glutamate challenge

After 24h of seeding, HT4 cells were transfected with adenoviral vector containing the glutaredoxin 1 (ad-GRx1) cDNA construct with dose-dependent manner. (**A**, Western blot; **B–C**, immunocytochemistry, blue-DAPI stained nuclei; green-GRx1 protein; **B**, cells transfected with 2000 m.o.i ad-LacZ; **C**, cells tranfected with 2000 m.o.i ad-GRx1). **D**, after transfection with ad-LacZ or ad-GRx1 (2000 m.o.i), HT4 cell lysates (30μg) were subjected to SDS-PAGE and immunoblotting for the detection of formation of glutathionylation. HT4 cells transfected with ad-GRx1 expressed lower formation of glutathionylation; **E**, HT4 cells were transfected ad-LacZ or ad-GRx1. After 72h of transfection, cells were re-split and incubated for 24h. Cells were challenged with or without 10mM glutamate for 24h, and viability of HT4 cells were assessed by measuring leakage of lactate dehydrogenase (LDH). Cells overexpressing GRx1 were more resistant to glutamate-induced loss of cell viability. **F**, After transfection with 12-Lox containing V5 epitope, HT4 cells were challenged with 10mM glutamate for 8h. Cell lysates (500μg) were subjected to IP with V5 antibody. IP were subjected to SDS-PAGE and immunoblotting for the detection of formation of glutathionylation. Cells treated with glutamate expressed higher formation of GSS-12-Lox. However, in GRx1 transfected cells glutamate-induced 12-Lox glutathionylation was blunted. n=3, Bar, 50 μm. *, higher than control, †, lower than glutamate-challenged LacZ. Results are mean ± S.D. *, $p < 0.05$.
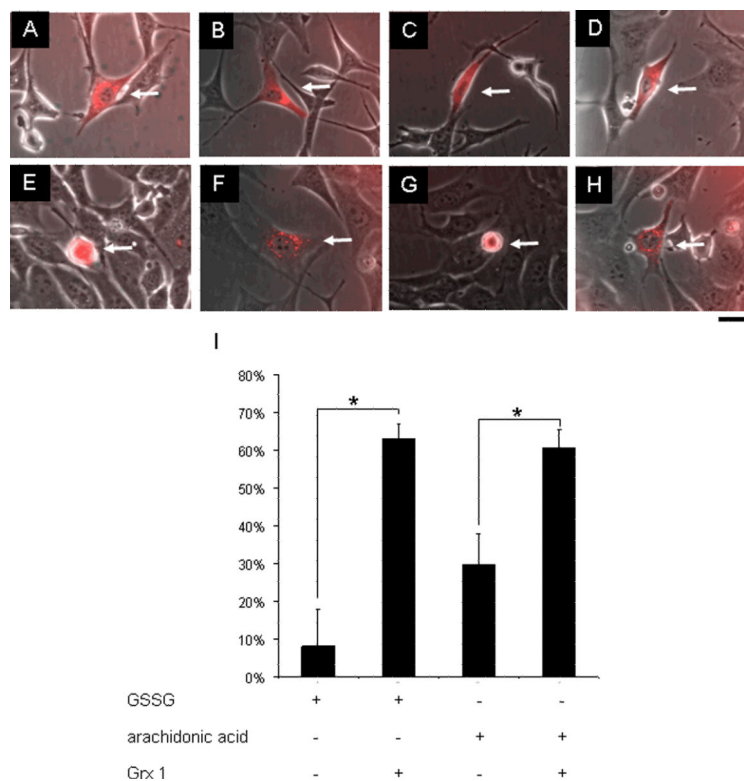
Figure 9. Glutaredoxin-1 microinjection protected HT4 neural cells against GSSG as well as arachidonic acid challenge

Cultured HT4 cells were either injected 500 attomole GSSG (**A** and **B**) or 0.15 attomole arachidonic acid (**C** and **D**), and co-injected with 2 attomole glutaredoxin-1 (**B** and **D**). After 24h incubation, cells injected with GSSG (**E**) lost cell viability, while glutaredoxin-1 co-injected cells (**F**) were significantly protected. Cells injected with arachidonic acid (**G**) lost cell viability, while glutaredoxin 1 co-injected cells (**H**) were protected (**I**). attomoles injected [micromolar]i, n=3, Bar, 20 μm. Results are mean ± S.D. *, $p < 0.05$.
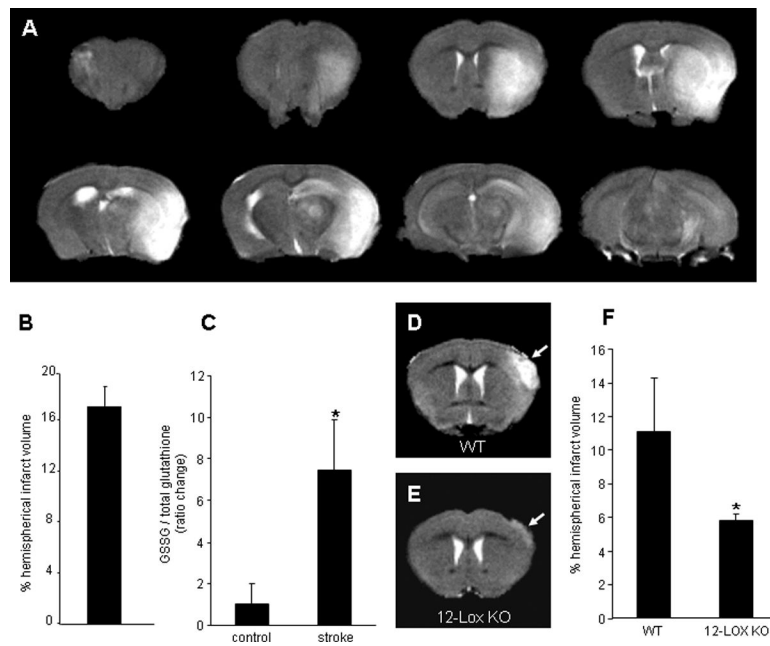
Figure 10. 12-Lipoxygenase-deficient mice were resistant to GSSG-induced brain damage
Transient focal cerebral ischemia was induced in 8 to 10 week old C57BL6/J mice (n=3) by middle cerebral artery occlusion for 90 min. **A**, Brain infarction was detected by T2-weighted MRI images at 24h after reperfusion. **B**, MRI images were used to determine infarct size as a percentage of the hemispherical infract volume. **C**, HPLC coulometric electrode array detector was used to detect GSSG and GSH level in the infarcted tissue, and stroke-induced injured hemisphere contained elevated level of GSSG. GSSG was injected to the brain cortex of C57BL6/J (control, n=3) or 12-Lox knock-out (12-Lox$^{-/-}$, n=3) mice. Two days after injection, T2-weighted MRI images were collected. WT mice injected with GSSG (**D**) had clear lesion in the brain while 12-Lox deficient mice (**E**) were significantly resistant to GSSG-induced brain injury (**F**). Solid arrows represent damage caused by GSSG. Results are mean ± S.D. *, $p < 0.05$.